

## GENERATION OF ORTHONORMAL-CRACK-PATTERN IMAGES BY MINIMUM/MAXIMUM FILTERING

TORU HIRAOKA

Department of Information Systems  
University of Nagasaki  
1-1-1, Manabino, Nagayo-chou, Nishisonogi-gun, Nagasaki-ken 851-2195, Japan  
hiraoka@sun.ac.jp

Received July 2019; accepted October 2019

**ABSTRACT.** *This paper presents a non-photorealistic rendering (NPR) method for generating orthonormal-crack-pattern images (OCP images) from photographic images. OCP images are non-photorealistic images obtained by overlaying orthonormal-crack-patterns on photographic images. The proposed method is executed by an iterative calculation using minimum/maximum filtering. The proposed method is simple and easy to implement, and can generate orthonormal-crack-patterns by preserving the edges of photographic images. In order to validate the effectiveness of the proposed method, experiments using various photographic images are conducted. Results show that the proposed method can generate impressive OCP images in which the edges are preserved.*

**Keywords:** Non-photorealistic rendering, Orthonormal-crack-pattern, Minimum/maximum filtering, Automatic generation, Iterative calculation

1. **Introduction.** Image processing technology [1, 2, 3] is widely used in the field of computer graphics. NPR is a technique of computer graphics that focuses on expressing various styles of digital art [4, 5, 6, 7, 8, 9]. NPR systems take photographic images, animations, videos or three-dimensional models as input, and then give users non-photorealistic images as output. Although users of NPR have been professional creators in the field of movies, television and video games, NPR implemented in personal computer and smart phone applications is made easy for general users in recent years. At the same time, NPR with unprecedented expressions are required by general users and professional creators.

This paper proposes a novel NPR method for generating OCP images from photographic images as an expression method of NPR which has not existed so far. OCP images are non-photorealistic images embedded in many orthonormal-crack-patterns to photographic images. The proposed method is executed by an iterative calculation using minimum/maximum filtering, so it is simple to process and easy to implement. The feature of the proposed method is that orthonormal-crack-patterns can be automatically generated while preserving the edges of photographic images. In order to visually verify the effectiveness of the proposed method, an experiment using Lenna image is conducted to investigate the changes of orthonormal-crack-patterns generated by varying the values of the parameters in the proposed method. In addition, the proposed method is applied to various images. As a result of the experiments, it is revealed that orthonormal-crack-patterns can be automatically generated on the whole image.

Studies to express crack patterns have been conducted [10, 11, 12]. Wyvill et al. proposed a method for simulating the cracks found in Batik wax painting and dyeing technique used to make images on cloth by distance transform algorithm [10]. Jing and Urahama proposed a method for generating line-guided crack images by Apollonius tessellation [11]. Iben and O'Brien proposed a method for generating surface crack patterns

that appear in materials such as mud, ceramic glaze and glass by physical simulation [12]. These conventional methods are difficult to implement and computationally costly. In contrast, the proposed method is simple to implement and has low computing cost. Also, orthonormal-crack-patterns of the proposed method are different from the patterns of the conventional methods.

The rest of this paper is organized as follows. Section 2 describes the proposed method for generating OCP images. Section 3 shows experimental results, and reveals the effectiveness of the proposed method. Finally, Section 4 concludes this paper.

**2. Proposed Method.** The proposed method generates OCP images from photographic images. The proposed method is executed by the iterative calculation using minimum/maximum filtering. A flow chart of the proposed method is shown in Figure 1. In Step 1 of Figure 1, minimum and maximum values in the differences between the target pixel and the surrounding pixels are calculated. In Step 2, the minimum or maximum differences are added to photographic images. In Step 3, the averages of the minimum and maximum differences are added to photographic images. Therefore, the proposed method is simple without difficult processing.

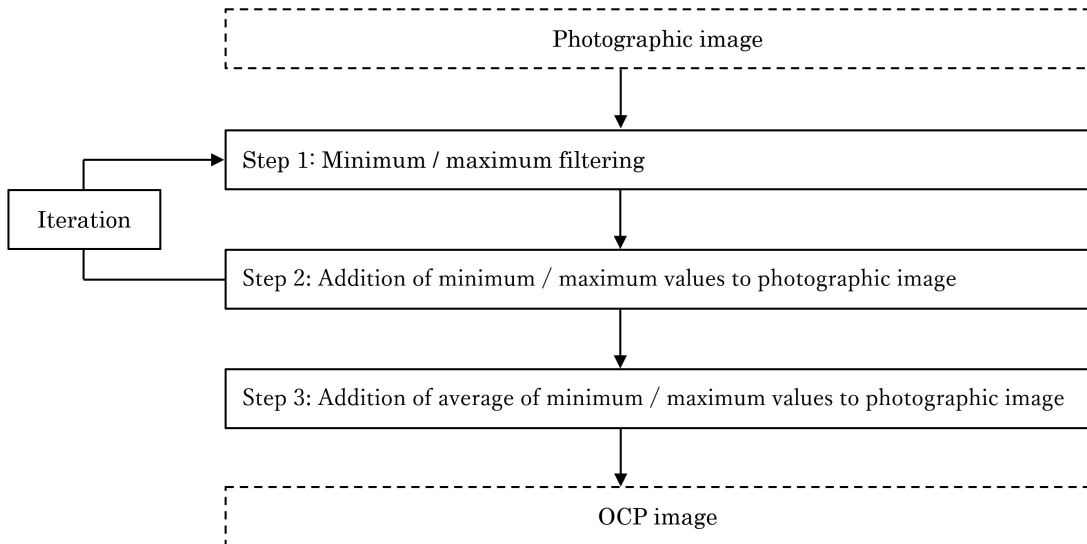


FIGURE 1. Flow chart of the proposed method

The input pixel values for spatial coordinates  $(i, j)$  of a gray-scale photographic image are established as  $f_{i,j}$ . The output pixel values by minimum/maximum filtering are computed as  $f_{i,j}^{(t)}$ , where  $t$  is the iteration number and  $f_{i,j}^{(0)} = f_{i,j}$ . The pixel values of  $f_{i,j}$  and  $f_{i,j}^{(t)}$  have value of  $M$  gradation from 0 to  $M - 1$ . Detailed procedure of the proposed method is shown below.

**Step 1:** The differences  $d_{i,j,k,l}^{(t)}$  are obtained by Equation (1).

$$d_{i,j,k,l}^{(t)} = f_{i,j}^{(t-1)} - f_{k,l}^{(t-1)} \quad (1)$$

where the coordinates  $(k, l)$  are positions included within  $\pm W$  around the coordinates  $(i, j)$ , where  $W$  is window size and a positive constant. Minimum and maximum values in  $d_{i,j,k,l}^{(t)}$  are established as  $d_{\min,i,j}^{(t)}$  and  $d_{\max,i,j}^{(t)}$ , respectively.

**Step 2:** The pixel values  $f_{i,j}^{(t)}$  are calculated by Equation (2).

$$f_{i,j}^{(t)} = \begin{cases} f_{i,j} + d_{\min,i,j}^{(t)} & (t \text{ modulo } 2 = 0) \\ f_{i,j} + d_{\max,i,j}^{(t)} & (t \text{ modulo } 2 = 1) \end{cases} \quad (2)$$

where  $f_{i,j}^{(t)}$  must be set to 0 in case  $f_{i,j}^{(t)}$  is less than 0, and  $f_{i,j}^{(t)}$  must be set to  $M - 1$  in case  $f_{i,j}^{(t)}$  is greater than  $M - 1$ . In Equation (2), when  $t$  is an even number,  $d_{\min,i,j}^{(t)}$  are added to  $f_{i,j}$ , and when  $t$  is an odd number,  $d_{\max,i,j}^{(t)}$  are added to  $f_{i,j}$ . Steps 1 and 2 are repeated  $T$  times.

**Step 3:** The pixel values  $F_{i,j}$  are calculated by Equation (3).

$$F_{i,j} = f_{i,j} + \frac{d_{\min,i,j}^{(T)} + d_{\max,i,j}^{(T)}}{2} \quad (3)$$

In Equation (3), the averages of  $d_{\min,i,j}^{(t)}$  and  $d_{\max,i,j}^{(t)}$  are added to  $f_{i,j}$ . An image constituted by  $F_{i,j}$  is an OCP image. Orthonormal-crack-patterns are expressed darker if  $T$  is an even number, and are done brighter if  $T$  is an odd number.

**3. Experiments.** Two experiments were conducted. In the first experiment, the values of the parameters were changed and the appearances of OCP images were visually confirmed. In the second experiment, the appearance of OCP images was visually confirmed using various photographic images.

**3.1. Experiment with changing parameters.** The proposed method was applied to Lenna image (Figure 2) with  $512 \times 512$  size and 256 gradation. The changes in appearance to OCP images were visually assessed as the values of the parameters  $W$  and  $T$  were varied. The value of  $W$  was varied to 1, 2, 3 and 4, and  $T$  was varied to 99 and 100. The reason for setting  $T$  to 99 and 100 is because OCP images converged and orthonormal-crack-patterns did not change. The OCP images for  $W = 1, 2, 3$  and 4 and  $T = 99$  are shown in Figure 3. The OCP images for  $W = 1, 2, 3$  and 4 and  $T = 100$  are shown in Figure 4. As shown, as  $W$  became smaller, orthonormal-crack-patterns became finer. The value of  $W$  may be set according to the application of the user. Orthonormal crack patterns became darker if  $T$  was an even number ( $T = 99$ ), and became brighter if  $T$  was an odd number ( $T = 100$ ).



FIGURE 2. Lenna image

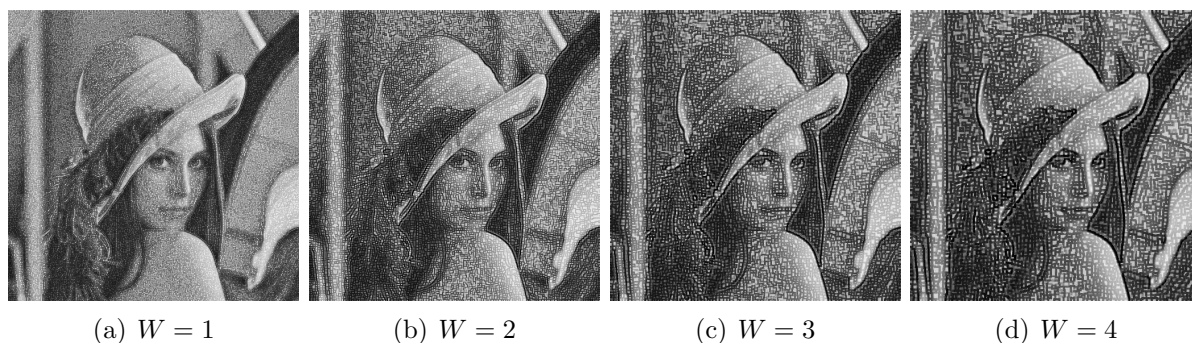


FIGURE 3. OCP images for  $W = 1, 2, 3$  and 4 and  $T = 99$

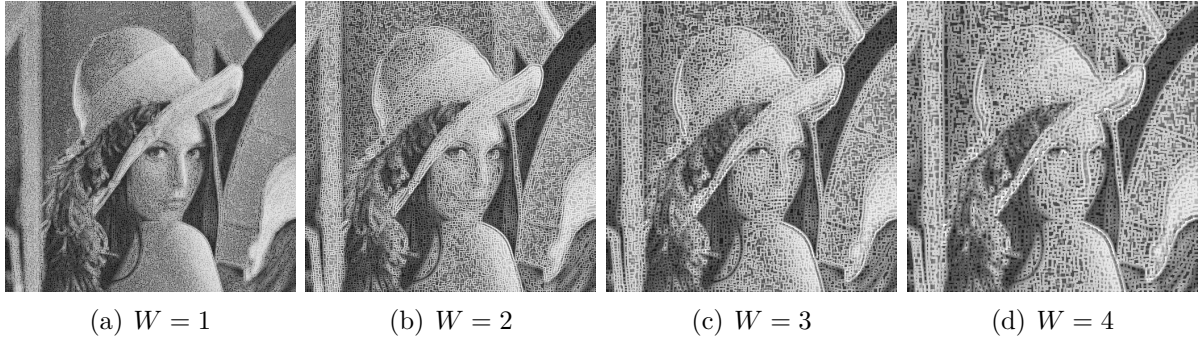


FIGURE 4. OCP images for  $W = 1, 2, 3$  and  $4$  and  $T = 100$

**3.2. Experiment using various photographic images.** The proposed method was applied to eight photographic images with  $512 \times 512$  size and 256 gradation besides Lena image. Eight photographic images are shown in Figure 5. The values of  $W$  and  $T$  were set to 2 and 99, respectively. The reason for setting  $W$  and  $T$  to be 2 and 99 is because orthonormal-crack-patterns were relatively easy to recognize in the previous experiment. The results are shown in Figure 6. In all cases, orthonormal-crack-patterns could be automatically generated while preserving the edges of photographic images. However, orthonormal-crack-patterns were less likely to occur in white and black areas.



FIGURE 5. Various photographic images

**4. Conclusions.** This paper proposed a novel NPR method for generating OCP images from gray-scale photographic images by an iterative calculation using minimum/maximum filtering. The proposed method had features that the processing is simple and orthonormal-crack-patterns can be automatically generated by preserving the edges of photographic images. In the experiments using Lenna image and other photographic images, it was clarified that the proposed method can practically realize these features. However, it was found out that orthonormal-crack-patterns are less likely to occur in white and black areas.

A subject for future study is to be able to generate orthonormal-crack-patterns in white and black areas. Another task is to expand the proposed method for application to color photographic images.

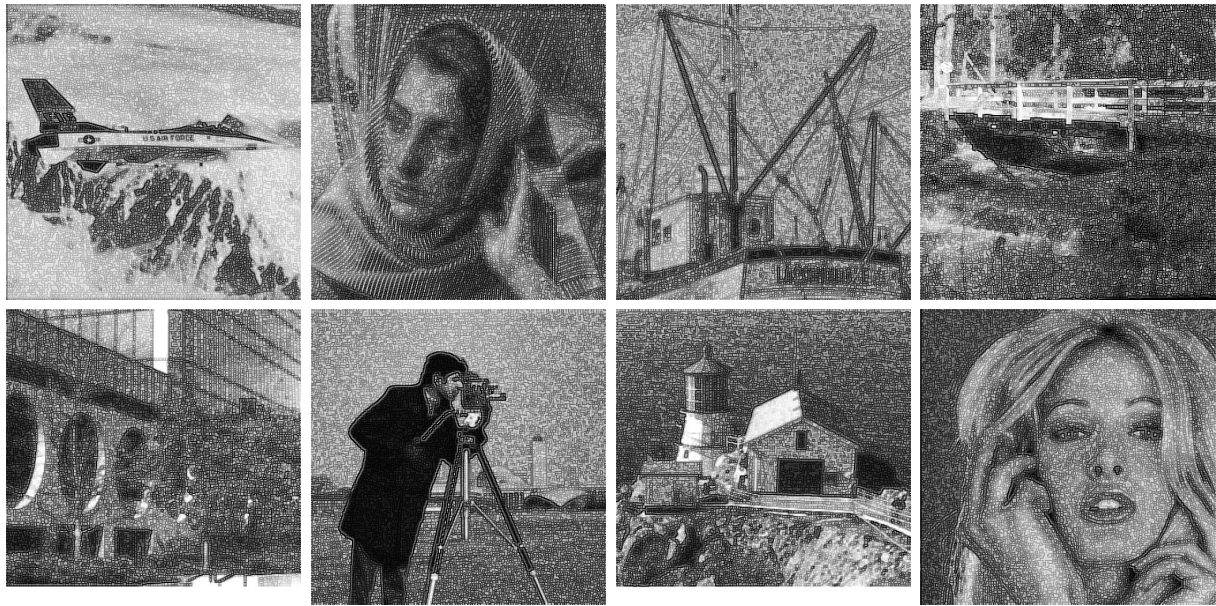


FIGURE 6. OCP images

## REFERENCES

- [1] P. Maniriho and T. Ahmad, High quality PVM based reversible data hiding method for digital images, *International Journal of Innovative Computing, Information and Control*, vol.15, no.2, pp.667-680, 2019.
- [2] R. Matsumura and A. Hanazawa, Human detection using color contrast-based histograms of oriented gradients, *International Journal of Innovative Computing, Information and Control*, vol.15, no.4, pp.1211-1222, 2019.
- [3] H. Yang, W. Gan, F. Chen and X. Li, Face recognition using shearlets edges fusion, *International Journal of Innovative Computing, Information and Control*, vol.15, no.4, pp.1309-1322, 2019.
- [4] J. Daniel, S. Erik, Y. Anders and R. Timo, A survey of volumetric illumination techniques for interactive volume rendering, *Computer Graphics Forum*, vol.33, no.1, pp.27-51, 2014.
- [5] L. A. Gatys, A. S. Ecker and M. Bethge, Image style transfer using convolutional neural networks, *The IEEE Conference on Computer Vision and Pattern Recognition*, pp.2414-2423, 2016.
- [6] W. Qian, D. Xu, K. Yue, Z. Guan, Y. Pu and Y. Shi, Gourd pyrography art simulating based on non-photorealistic rendering, *Multimedia Tools and Applications*, vol.76, no.13, pp.14559-14579, 2017.
- [7] D. Martin, G. Arroyo, A. Rodriguez and T. Isenberg, A survey of digital stippling, *Computers & Graphics*, vol.67, pp.24-44, 2017.
- [8] T. Wu, Saliency-aware generative art, *Proc. of the 10th International Conference on Machine Learning and Computing*, pp.198-202, 2018.
- [9] L. Scalera, S. Seriani, A. Gasparetto and P. Gallina, Non-photorealistic rendering techniques for artistic robotic painting, *Robotics*, vol.8, no.1, 2019.
- [10] B. Wyvill, K. V. Overveld and S. Carpendale, Rendering cracks in Batik, *Proc. of the 3rd International Symposium on Non-Photorealistic Animation and Rendering*, pp.61-149, 2004.
- [11] L. Jing and K. Urahama, Line-guided cracks image with apollonius tessellation, *IEICE Transactions*, vol.89-A, no.10, pp.849-851, 2006.
- [12] H. N. Iben and J. F. O'Brien, Generating surface crack patterns, *Graphical Models*, vol.71, no.6, pp.198-208, 2009.